

# Position control for the MSL Kibble balance coil using a syringe pump

Rebecca J. Hawke<sup>1</sup>, Mark T. Clarkson<sup>1</sup>

<sup>1</sup> Measurement Standards Laboratory (MSL), Lower Hutt, New Zealand

## ABSTRACT

The position of the coil in a Kibble balance must be finely controlled. In weighing mode, the coil remains stationary in a location of constant magnetic field. In calibration mode, the coil is moved in the magnetic field to induce a voltage. The MSL Kibble balance design is based on a twin pressure balance where the coil is attached to the piston of one of the pressure balances. Here we investigate how the piston (and therefore coil) position may be controlled through careful manipulation of the gas column under the piston. We demonstrate the use of a syringe pump as a programmable volume regulator which can provide fall rate compensation as well as controlled motion of the piston. We show that the damped harmonic oscillator response of the pressure balance must be considered when moving the coil. From this initial investigation, we discuss the implications for use in the MSL Kibble balance.

Section: RESEARCH PAPER

Keywords: Kibble balance; pressure balance; position control; volume control

Citation: Rebecca J. Hawke, Mark T. Clarkson, Position control for the MSL Kibble balance coil using a syringe pump, Acta IMEKO, vol. 11, no. 4, article 16, December 2022, identifier: IMEKO-ACTA-11 (2022)-04-16

Section Editor: Andy Knott, National Physical Laboratory, United Kingdom

Received July 11, 2022; In final form October 5, 2022; Published December 2022

Copyright: This is an open-access article distributed under the terms of the Creative Commons Attribution 3.0 License, which permits unrestricted use, distribution, and reproduction in any medium, provided the original author and source are credited.

Funding: This work was supported by the New Zealand Government.

Corresponding author: Rebecca Hawke, e-mail: [rebecca.hawke@measurement.govt.nz](mailto:rebecca.hawke@measurement.govt.nz)

## 1. INTRODUCTION

Following the revision of the SI, Kibble balances around the world may now be used to realise the unit of mass. [1] In a Kibble balance, the weight of a mass is balanced by the electromagnetic force on a current-carrying coil of wire suspended in a magnetic field. At MSL we are developing a Kibble balance where the coil is connected to the piston of pressure balance 1 (see Figure 1) in a twin pressure balance arrangement [2], [3]. The piston-cylinder unit of pressure balance 1 provides a repeatable axis for the motion of the coil in the magnetic field. The twin pressure balance arrangement serves as a high-sensitivity force comparator, [4].

In a Kibble balance, the position of the coil must be precisely controlled in both weighing and calibration modes. In weighing mode the coil should remain stationary at a set position while the current is adjusted to maintain a force balance. In the MSL Kibble balance, stability in position to within  $1\ \mu\text{m}$  would correspond to an uncertainty in realised mass of 3.5 parts in  $10^9$ , [5]. In calibration mode, the coil must be moved such that a measurable voltage is induced, which typically requires velocities between  $1.3\ \text{mm s}^{-1}$  and  $3\ \text{mm s}^{-1}$ , [6]. In the MSL Kibble

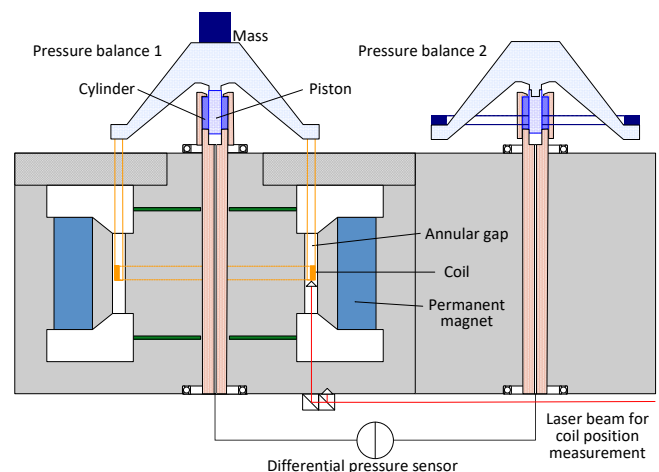


Figure 1. Schematic of the MSL Kibble balance design based on a twin pressure balance. The coil connects to the piston of pressure balance 1 such that the coil and magnet are coaxial with the piston-cylinder unit. Pressure balance 2 provides a reference pressure for a differential pressure sensor to determine changes in balance forces.

balance, control of the vertical position of the coil equates to control of the piston position in pressure balance 1. However, in a pressure balance the piston naturally falls as gas leaks through the annular gap between piston and cylinder. Fall rate compensation is therefore necessary in both weighing and calibration modes in the absence of mechanical controls such as arresting stops or a direct motor drive.

To assist in control of the coil position in the MSL Kibble balance, we propose careful manipulation of the gas column under the piston in pressure balance 1. The pressure balance maintains a constant pressure, so our options are to adjust the gas volume (e.g. with a mass flow controller) or to shift the gas column in space (e.g. with a volume regulator). To test this second approach to coil position control, we investigate the use of a syringe pump as an automated volume regulator. The layout of this paper is as follows. In Section 2 we describe the experimental apparatus, and in Section 3 we propose a theoretical model for the system. Results for fall rate compensation, conventional constant velocity travel, and an oscillatory motion are presented in Section 4. Finally, in Section 5 we discuss the potential for this technique to be used in the MSL Kibble balance.

## 2. EXPERIMENTAL APPARATUS

The experimental apparatus is illustrated in Figure 2 and was similar to that used in [8].

The pressure balance was a pneumatic DHI/Fluke 50 kPa/kg piston-cylinder module with an effective area of 196 mm<sup>2</sup>. The medium was zero grade nitrogen gas and we adjusted the load to give a working pressure near 100 kPa absolute. We used a manual volume controller to set the initial height of the piston. The pressure balance was operated in a vacuum chamber evacuated to a pressure of around 0.1 Pa. Ambient temperature outside the chamber was in the range 21 – 23 °C during measurements.

To control the vertical position of the piston, we used a custom ‘Direct Drive’ model of the Cetoni Nemesys S syringe pump. This pump has inbuilt position encoding. Cetoni high-precision glass syringes of 1 mL, 5 mL and/or 25 mL capacity were connected to the pressure balance via 1 m of 1/8” flexible PTFE tubing (1.6 mm ID) and a minimal length of 1/4” Swagelok stainless steel tubing and fittings. We estimate the smallest

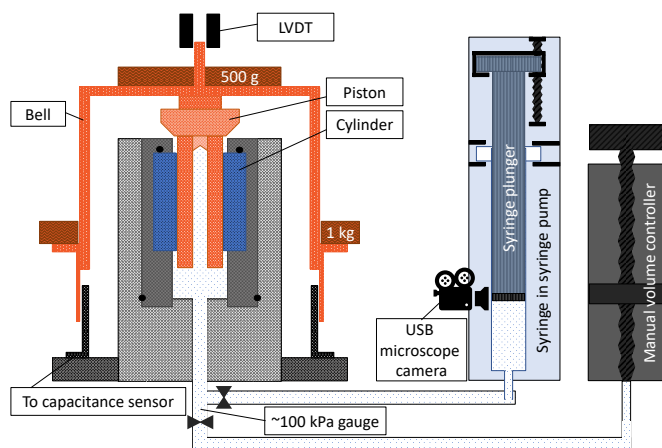


Figure 2. Schematic of the experimental apparatus for piston position control using a syringe in a syringe pump as a volume regulator. Floating elements are coloured orange. Not shown are the drive mechanism for starting piston rotation (see [7]), the support for the LVDT, and the vacuum chamber surrounding the pressure balance.

volume of the gas column was ~30 mL including the cavity within the piston.

To enable rapid, independent tracking of the syringe volume, we monitored the position of the syringe plunger using an IDS uEye USB camera with a microscope lens attached. We converted the image pixels to volume in mL for each syringe using the encoder values at eight positions spanning the range of travel. To determine the phase shift or delay between syringe plunger motion and piston motion we used hardware triggering of the image capture and piston position measurements. However, triggering increased the measurement noise, so data shown here were captured using the camera’s free-run mode.

We measured the piston position using both a capacitance sensor and a linear variable differential transducer (LVDT) with hardware triggering at either 20 or 50 ms intervals. We determined the calibration curve for the capacitor using a dial gauge and gauge blocks and transferred the calibrated position to the LVDT readings. The results presented use the LVDT readings.

## 3. MODEL

A gas pressure balance comprises a loaded piston floating on a volume of gas, and behaves as a damped harmonic oscillator, [8], [9]. A pressure balance connected to a syringe has a mechanical analogue in the accelerometer (or seismometer). Figure 3 illustrates this model, where the loaded piston ‘mass’ is attached to a syringe plunger ‘platform’ by a gas pressure ‘spring’, with ‘dashpot’ damping. Moving the platform moves the mass in a linear motion with coupled oscillations described by the equation of motion:

$$-\ddot{z}' = \ddot{z}_r + \frac{c}{m} \dot{z}_r + \omega_0^2 z_r, \quad (1)$$

where  $z_r$  is the relative distance between mass  $m$  and platform,  $z'$  is the displacement of the platform,  $c$  is the damping coefficient, and  $\omega_0$  is the resonant frequency. Dots indicate derivatives with respect to time.

In a pressure balance, the resonant frequency depends on the volume of the gas column under the piston. In the experimental configuration here, the resonant frequency can be varied from ~0.5 Hz to 1.2 Hz. Both the resonant frequency and the ratio  $\frac{c}{m}$  may be obtained from the damped natural oscillations of the system.

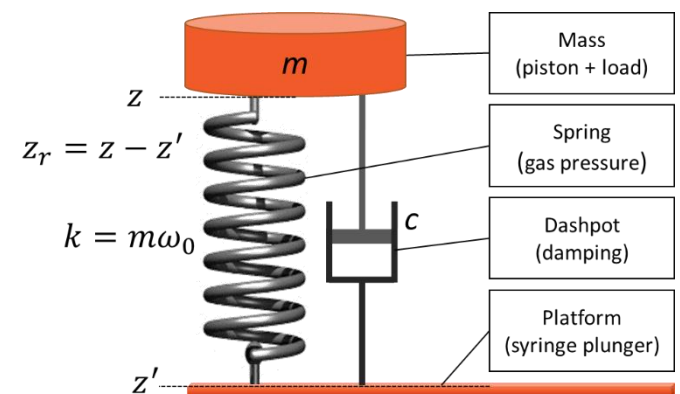


Figure 3. Accelerometer model of a pressure balance when connected to a syringe in a syringe pump. The loaded piston ‘mass’ is attached to a syringe plunger ‘platform’ by a gas pressure ‘spring’, with ‘dashpot’ damping.

This system can be driven with a sinusoidal motion of the platform. For a driving displacement  $z'(t) = A_0 \cos(\omega t)$  with amplitude  $A_0$  and frequency  $\omega$ , the equation of motion has a solution of the form:

$$z_r(t) = A_{el} \cos(\omega t) + A_{inel} \sin(\omega t). \quad (2)$$

Solving for the coefficients gives the elastic coefficient,

$$A_{el} = \frac{A_0 \omega^2 (\omega_0^2 - \omega^2)}{(\omega_0^2 - \omega^2)^2 + \left(\frac{c}{m} \omega\right)^2}, \quad (3)$$

and the inelastic coefficient,

$$A_{inel} = \frac{A_0 \frac{c}{m} \omega^3}{(\omega_0^2 - \omega^2)^2 + \left(\frac{c}{m} \omega\right)^2}. \quad (4)$$

The behaviour of the driven system can be understood by examining these coefficients at their limits. As the driving frequency  $\omega$  tends to 0, the amplitude of  $z_r$  tends to 0, and the motion of the mass,  $z$ , follows the motion of the platform:

$$z(t) = z'(t) + z_r(t) = A_0 \cos(\omega t). \quad (5)$$

As the driving frequency tends to infinity,  $A_{el}$  tends to  $-A_0$  and  $A_{inel}$  tends to 0, such that the mass remains stationary despite the motion of the platform:

$$z(t) = z'(t) + z_r(t) = A_0 \cos(\omega t) - A_0 \cos(\omega t) = 0. \quad (6)$$

In between these limits, for  $\frac{c}{m} < \omega_0$  the amplitude of  $z_r$  reaches a maximum as the driving frequency approaches the resonant frequency. At resonance,  $A_{el}$  tends to 0 and the motion of the mass is approximately  $90^\circ$  behind the driving oscillation  $z'$ :

$$z(t) = z'(t) + z_r(t) = A_0 \cos(\omega_0 t) + A_0 Q \sin(\omega_0 t) \quad (7)$$

where  $Q = \frac{m}{c} \omega_0$  is the quality factor of the damped natural oscillations of the system.

## 4. RESULTS

### 4.1 Fall rate compensation

When used in a Kibble balance in weighing mode, over the course of several ‘mass-on, mass-off measurements’ the natural fall rate of the piston of around  $1 \mu\text{m s}^{-1}$  would result in a significant change in piston position. However, for the lowest uncertainty, the weighing position should be kept constant between loadings. Here we consider the usefulness of a syringe pump to maintain a steady piston position by providing a very low flow to compensate for the natural fall of the piston.

In Figure 4 we show a typical fall rate compensation test using a constant flow rate of  $0.012 \text{ ccm}$  ( $\text{ccm} = \text{cm}^3 \text{ min}^{-1}$ ). Initially, while the syringe volume is kept constant, the piston falls at an average rate of  $1.004 \mu\text{m s}^{-1}$  over 5 minutes. The syringe plunger is then moved slowly, shifting the column of gas towards the piston and causing a slight rise of  $0.015 \mu\text{m s}^{-1}$  over the ten minutes of applied flow. When the syringe plunger motion is stopped, the piston returns to falling, this time at  $0.986 \mu\text{m s}^{-1}$  over 5 minutes. This fall compensation resulted in a rise in the piston position of  $8.9 \mu\text{m}$  over ten minutes.

Over several flow rate compensation tests we observed some variation in the fall rate of the piston. Within a test, the fall rate varied before and after fall compensation by up to  $0.06 \mu\text{m s}^{-1}$ ,

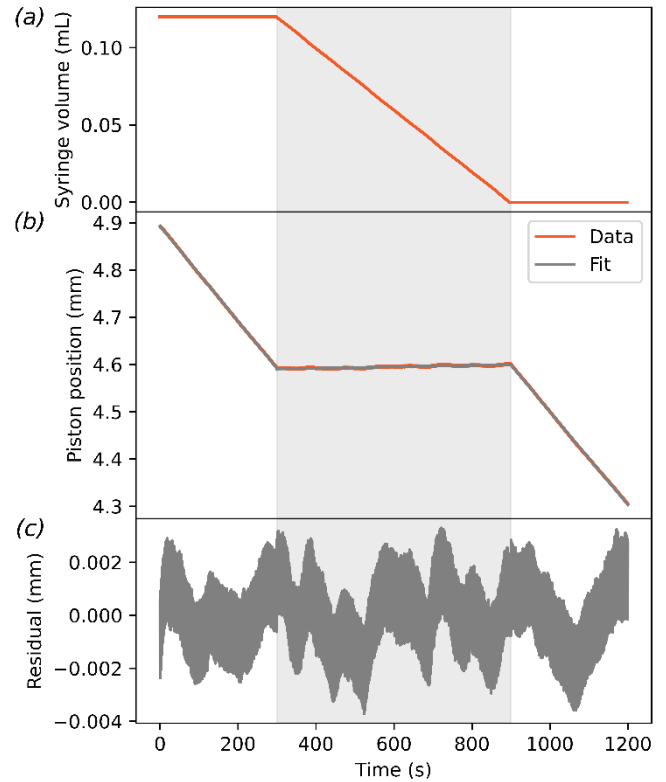


Figure 4. Fall rate compensation using a flow rate of  $0.012 \text{ ccm}$  for ten minutes (grey shaded region). (a) The syringe plunger motion is linear in the shaded region. (b) The piston position is maintained with the  $0.012 \text{ ccm}$  flow, and falls at its natural fall rate outside of the shaded region (c) Residuals are from a linear fit in each region.

and between tests the variation was at most  $0.28 \mu\text{m s}^{-1}$ . During fall compensation with the same nominal flow rate of  $0.012 \text{ ccm}$  at the syringe plunger, the overall change in piston position varied between falling by  $11 \mu\text{m}$  over ten minutes when the initial fall rate was  $1.13 \mu\text{m s}^{-1}$ , and rising by  $80 \mu\text{m}$  over the same time when the initial fall rate was  $0.86 \mu\text{m s}^{-1}$ . In the latter case, a subsequent test with a constant flow rate of  $0.011 \text{ ccm}$  resulted in a rise in the piston position of  $2 \mu\text{m}$  after ten minutes.

The start and stop of the syringe plunger motion is a disturbance to the piston. However, the size of this disturbance is very small, and no resonant behaviour is observable. Also, we would expect very little disturbance from the syringe plunger when in motion as these flow rates are in the pulsation-free regime of the syringe pump when using a  $1 \text{ mL}$  syringe. Instead, we observe some random variation in piston position of up to  $2 \mu\text{m}$ , which may be due to temperature fluctuations in the gas or external disturbances as they are also seen when the piston is falling without flow compensation.

### 4.2 Calibration mode – constant velocity

In calibration mode in most existing Kibble balances, the coil is typically moved through the weighing position at an approximately constant velocity of between  $1.3 \text{ mm s}^{-1}$  and  $3 \text{ mm s}^{-1}$ , [6]. With the experimental configuration in Figure 2, these velocities are achievable with flow rates between  $15 \text{ ccm}$  and  $35 \text{ ccm}$ . However, unlike in the case of leak compensation, the abrupt start and stop of the syringe plunger during this rapid motion is a significant disturbance which causes a visible damped oscillator response.

Figure 5 shows the shape of the travel for an intermediate flow rate of  $20 \text{ ccm}$ . Immediately after the travel region, we see

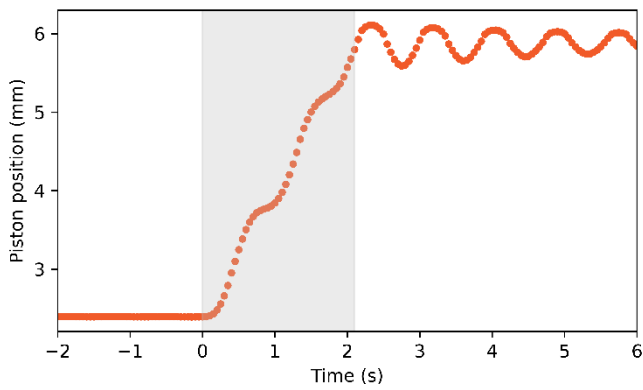


Figure 5. Shape of the piston travel for a 0.7 mL volume change at 20 ccm which gives an effective velocity of  $1.7 \text{ mm s}^{-1}$  in the travel region (shaded grey).

a damped harmonic oscillation; a similar oscillation is also superimposed onto the travel region. The weighing position will be at approximately the half-way point of the range of travel available. Although the piston moves through the weighing position quickly, the damped harmonic oscillation causes fluctuations in travel speed, with some very slow motion and even backward motion for some higher flow rates. The number of oscillations in the travel region depends on the time taken to complete the travel and the resonant frequency of the system. Here the system volume is as small as practicable, and the resonant frequency is around 1.2 Hz. Some improvement can be gained by reducing the resonant frequency of the system and timing the duration of the travel to match one period of the damped oscillation. However, the resulting instantaneous velocity is smoothly varying rather than constant during the travel.

Ideally, in constant velocity calibration mode the motion would have as close to zero acceleration as possible in the travel

region. We now present two controlled start techniques to suppress the harmonic oscillations. In the first technique, the flow is ramped up to the target flow and then ramped down when time to stop the motion. While the ‘ramp down’ step is not strictly necessary for our goal of constant velocity travel, the controlled deceleration reduces the damped oscillations after the travel. Minimising these oscillations maximises the range of available travel and minimises the settling time required before commencing the next traverse in the opposite direction.

Figure 6 (a) illustrates the syringe plunger motion for a gentle ramp up to 20 ccm, taking 0.76 s and travelling  $\sim 0.13 \text{ mL}$  per ramp. For a total volume change of 0.8 mL, the time spent at 20 ccm is 1.64 s in which the syringe plunger travels 0.547 mL. Note that in this plot the syringe plunger is moving to refill the syringe. Figure 6 (b) shows the resulting motion of the piston, which is significantly more linear than without the accelerating and decelerating ramps, for the same maximum flow rate. A three-section piecewise linear fit to the piston motion gives an average travel speed of  $1.72 \text{ mm s}^{-1}$  in the middle section. Residuals to this fit are shown in Figure 6 (c). Some disturbance is evident during each of the ramps, but the motion during the main travel section is linear to within  $\sim 33 \mu\text{m}$ . We note that the size of the observed variations will be influenced by integration of the signal within the sampling interval of 20 ms.

The second controlled start technique is known as the Crane Operator’s Trick, which exploits the natural oscillation period of the system, [10]. Implementing this trick here involves three steps of applied flow:

1. an initial step at half the target flow, for half a period of oscillation, to accelerate the piston,
2. a steady step at the target flow, to generate constant velocity travel, and
3. a final step of half the target flow, for half a period of oscillation, to decelerate the piston to stationary.

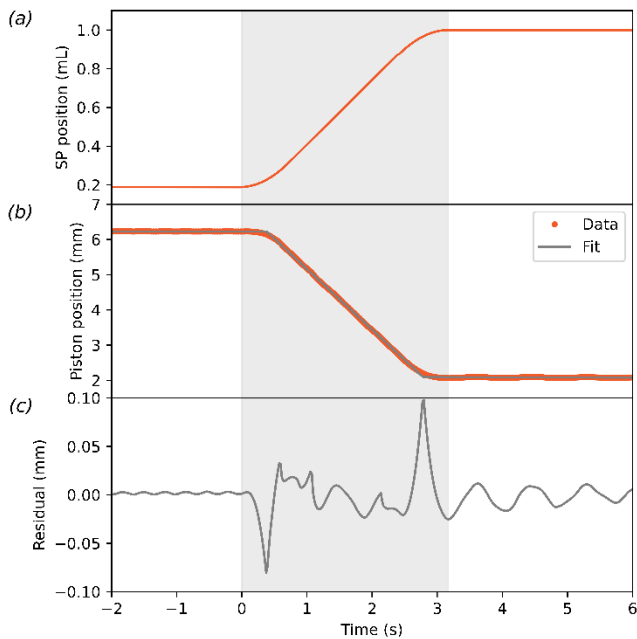


Figure 6. Constant velocity travel using gentle ramps over 0.76 s to a maximum flow of 20 ccm, for a 0.8 mL total volume change. (a) Shape of the syringe plunger motion (encoder values); the plunger is moving in the grey shaded region. (b) Resulting position of the piston (orange markers) and 3-piece linear fitting (grey line). (c) Residual to the piecewise linear fitting in (b).

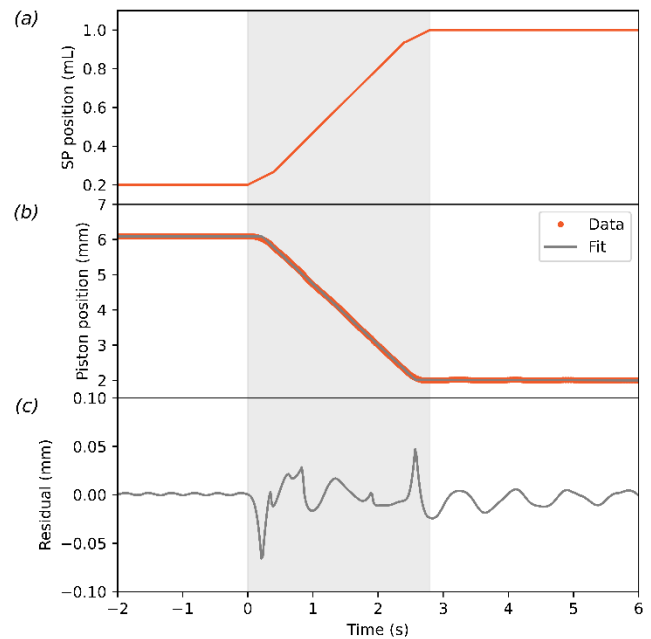


Figure 7. Constant velocity travel using the Crane Operator’s Trick with steps at 10 and 20 ccm for a 0.8 mL total volume change, with a period of 0.76 s. (a) Shape of the syringe plunger motion (encoder values); the plunger is moving in the grey shaded region. (b) Resulting position of the piston (orange markers) and 3-piece linear fitting (grey line). (c) Residual to fit in (b).

Figure 7 (a) shows these three distinct steps in the syringe plunger motion for a target flow of 20 ccm and total volume change of 0.8 mL. Each section at 10 ccm takes 0.38 s and travels only 0.063 mL, leaving 0.673 mL to travel at 20 ccm, over 2.02 s. The resulting motion of the piston is shown in Figure 7 (b), and residuals to a piecewise linear fit to the piston motion are shown in Figure 7 (c). The motion during the main travel section is linear to within  $\sim 29 \mu\text{m}$  with an average travel speed of  $1.73 \text{ mm s}^{-1}$ . The disturbance due to starting and stopping the syringe plunger is slightly less than for the ramp technique, and both techniques give very small damped oscillations after stopping the syringe plunger motion.

To provide sufficient data for the determination of the ratio of the induced voltage to the coil velocity at the weighing position, the coil is usually moved at a constant velocity over a distance of at least 20 mm, [6]. However, in the pressure balance that will be used for the MSL Kibble balance, the range of travel is restricted to at most 13 mm. This shorter range will therefore increase the number of repeats required to achieve the desired accuracy.

### 4.3 Calibration mode – oscillating velocity

As an alternative to the constant velocity method, an oscillatory motion has been suggested for the Kibble balance calibration mode, [6]. Sinusoidal oscillations with frequencies from 0.1 Hz to 5 Hz could be suitable, even with amplitudes as small as 1 mm. Oscillatory mode has been successfully implemented in the Ulusal Metroloji Enstitüsü (UME) Kibble balance by moving the magnet sinusoidally at a frequency of 0.5 Hz with a peak velocity of around  $3 \text{ mm s}^{-1}$ , [11]. Oscillatory mode has also been demonstrated in the ‘PB1’ and ‘PB2’ Planck-Balances where the optimal oscillation is typically 4 Hz with amplitudes of 4.5 and  $20 \mu\text{m}$  respectively, [12], [13]. In the MSL Kibble balance, a sinusoidal oscillation would work with (rather than against) the harmonic oscillator character of the pressure

balance. A suitable oscillation would have a frequency of around 1 Hz and an amplitude of  $\sim 1 \text{ mm}$ , [6].

Here we demonstrate driving such an oscillation via a sinusoidal displacement of the syringe plunger. The driving oscillation in syringe volume of 0.02 mL amplitude is shown in Figure 8 (a) along with the resulting piston oscillation in Figure 8 (b). For each dataset, we fit a single sinusoid to establish the frequency and amplitude. The frequency of the best fitting sinusoid was 0.9993 Hz for the syringe plunger motion and 0.9989 Hz for the piston motion. The resonant frequency of the system was adjusted to be as close to 1 Hz as practicable and was determined to be 0.9999 Hz from the damped harmonic oscillation after stopping the driving excitation. The amplitude of the piston oscillation was about 1.1 mm, with a peak velocity of around  $7.6 \text{ mm s}^{-1}$ . Assuming the induced voltage  $U = 1 \text{ V}$  for  $v = 2 \text{ mm s}^{-1}$ , we would expect this peak velocity to correspond to an induced voltage of almost 4 V when implemented in the MSL Kibble balance.

From our model we would expect the steady-state piston motion to lag behind the syringe plunger motion with a phase difference of  $90^\circ$ . This phase difference is evident here, where a reduction in syringe volume causes an upward motion of the piston.

Residuals to the sinusoidal fits are shown in Figure 8 (c), scaled by the respective amplitudes. We observe that there is periodic high frequency noise in the syringe plunger motion which is mostly filtered out by the pressure balance. However, the relative magnitude of the residual is transferred through to the piston motion and some non-sinusoidal periodic structure is evident.

Our accelerometer model for this scenario predicts an amplification of the piston oscillation when approaching the resonant frequency. In Figure 9 we present the model amplification due to a sinusoidal driving displacement, along with the measured amplitudes from a range of driving frequencies. We used the amplitude of the lowest frequency oscillation as the normalising amplitude value  $A_0$ . These data were collected using the smallest practical volume, giving a resonant frequency  $f_0$  of the system of around 1.175 Hz, determined by the damped harmonic oscillation after stopping

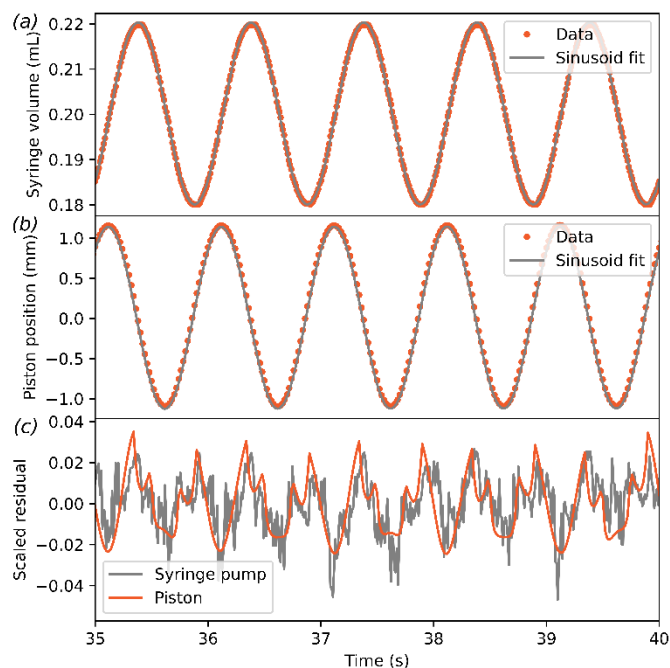


Figure 8. Oscillatory motion using a sinusoidal driving displacement at a frequency of 1 Hz. (a) Position of the syringe plunger. (b) Resulting position of the piston. (c) Residual to the best fitting sinusoids for (a) and (b), scaled by the respective amplitudes.

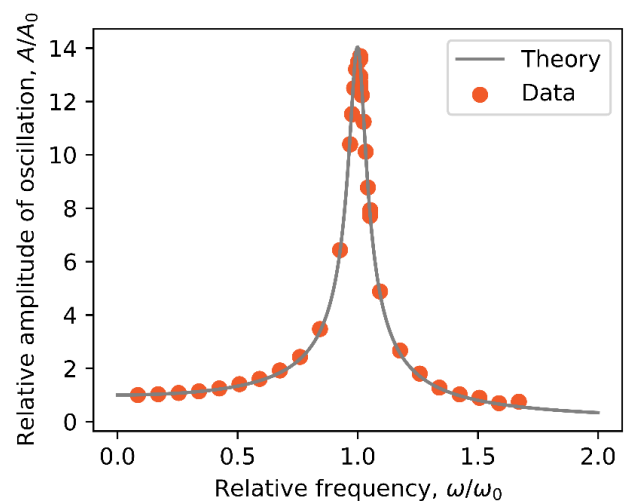


Figure 9. (orange markers) Amplitude of the piston motion resulting from a sinusoidal driving excitation of 0.025 mL amplitude at various frequencies, shown relative to the resonant frequency, and normalized to the amplitude at the lowest frequency. (grey line) Amplitude predicted by our model for a sinusoidal driving displacement, using  $Q = \frac{m}{c} \omega_0 = 14$  and  $f_0 = 1.175 \text{ Hz}$ .

the driving excitation. This damped harmonic oscillation had a quality factor of  $Q = \frac{m}{c} \omega_0 \sim 13$ , and the best fit model was obtained with a  $Q$  of 14.

## 5. DISCUSSION

### 5.1 Fall rate compensation

In the MSL Kibble Balance, fall rate compensation can supplement the use of a current feedback arrangement to control the coil position in weighing mode. Fall rate compensation will also be necessary for oscillatory mode if we use volume manipulation to generate the oscillation. From the results presented here, the use of a syringe pump to provide fall rate compensation is promising. The achieved  $5 \mu\text{m}$  stability over 5 minutes would be adequate for our initial target accuracy of 1 part in  $10^7$  for realised mass. To improve the obtained stability and the repeatability of the method, which are both limited by fluctuation in the piston fall rate, the fall rate should be measured immediately before each period of fall compensation to allow the ideal compensation flow rate to be determined. Alternatively, the flow could also be finely adjusted during an initial stabilisation routine.

We have examined possible causes, other than measurement error, of variations in the observed fall rate. Variation in the temperature of the piston-cylinder unit will affect the natural fall rate of the piston, through thermal expansion affecting the gap between piston and cylinder, and through the temperature dependence of the viscosity of the gas in the gap. For an estimated temperature change of 0.5 K of the piston-cylinder between measurements, these effects in terms of contribution to fall rate are calculated as being less than  $2 \text{ nm s}^{-1}$ . The fall rate is also expected to vary with vertical position of the piston due to departures from cylindricality of their shape. However, such a correlation is not evident in our data. A steady drift in temperature of the tubing connecting the pressure balance will affect the observed fall rate. For a 0.1 K change in temperature over 5 minutes, this effect is calculated to be  $\sim 7 \text{ nm s}^{-1}$  for a tubing volume of 35 mL and is mainly due to the section of PTFE tubing. This effect is an order of magnitude smaller than the variation in fall rate observed within a test. Similarly, the variation between tests of  $\sim 280 \text{ nm s}^{-1}$  is also unlikely to be due to the above causes. Instead, the variations may indicate that the tubing volume has a small leak which is influenced by changing ambient conditions.

Sources of the  $\sim 2 \mu\text{m}$  random variation in position should also be addressed. It is possible that this noise is due to ground vibration, or wobble from the spinning of the pressure balance bell. A rotating cylinder pressure balance is currently being developed which would provide a direct comparison and ideally lower noise.

This fall rate compensation technique is not only important for pressure balance 1 which carries the coil, but it can also be used for pressure balance 2 which is used to provide the reference pressure. Both pressure balances need to be kept at a stable pressure for the duration of weighing mode, which could take around 5 minutes per weighing. If left without fall compensation, pressure balance 2 would require periodic height adjustment. The height could easily be adjusted with the syringe pump before each weighing, and/or fall rate compensation could also be provided for this pressure balance throughout the duration of the weighing.

We note that this method could be considered to introduce a controlled leak into the system between the pressure balance and

the differential pressure transducer, which is not usually recommended, [14]. In this situation, the pressure in the tubing is very close to ambient pressure and the tubing volume is as small as practicable, which will reduce the effect of the leak. Additionally, the 'leak' caused by the motion of the syringe pump does not change the pressure or the number of gas molecules in the system; instead, the column of gas is merely moved along the tubing. For these reasons, we expect that the measured force difference would not be affected by a constant infusion during a weighing mode measurement consisting of a sequence of mass-on and mass-off weighings.

### 5.2 Constant velocity travel

As expected, the oscillator response of the pressure balance makes instantaneous travel at a constant velocity difficult to attain by simply applying a constant flow rate. Therefore, we have presented here two controlled start techniques which both significantly reduce the oscillator response. With these techniques, accommodating for the oscillator response took potentially as little as  $\sim 0.3 \text{ mm}$  at each end of the travel, out of the available travel of  $\sim 4 \text{ mm}$ . Of the two techniques, the Crane Operator's Trick is deceptively simple to implement, and produced constant velocity travel over almost the full range of travel of the piston with  $< 30 \mu\text{m}$  deviations from linear. Similar results were obtained for periods from 0.75 to 0.8 s, indicating that the exact timing of the steps is not critical. This technique warrants further investigation in the MSL Kibble Balance to enable interferometric velocity measurement and to assess the stability of the generated voltage.

### 5.3 Oscillating mode

In addition, we have demonstrated that volume manipulation can be used effectively to drive a sinusoidal oscillation of a pressure balance. We see good agreement with the nature of the driven oscillation at the piston and the features predicted by our model, such as a phase difference of  $90^\circ$  and a significant amplification near resonance. We postulate that there is likely to be only one mode of oscillation present due to the length of narrow tubing between syringe pump and piston.

The  $\sim 14$ -fold amplification of the driving oscillation near resonance is a major advantage in working with, rather than against, the harmonic oscillator character of the pressure balance. This amplification significantly reduces the amplitude of the driving oscillation that is required to generate an oscillation of  $\sim 1 \text{ mm}$  amplitude at the piston. Importantly, any noise in the driving oscillation is greatly reduced at frequencies above and below the resonant frequency. Care must be taken to reduce any noise in the driving oscillation at or near the resonant frequency, as this noise is also amplified.

The sinusoidal oscillation produced by our syringe pump is digitally created by updating the generated flow, 100 times per oscillation. This relatively coarse digitization results in a slightly distorted sinusoidal waveform, and the method of updating only the flow allows a slow drift of the average position of the plunger. While some optimisation is possible with the syringe pump system, a much better sinusoidal oscillation would be generated by an analogue or AC-driven input. Such an input could be used to drive the oscillation of the syringe plunger or an equivalent pressure-maintaining membrane or diaphragm.

Alternatively, a large, slow sinusoidal oscillation could be used to provide predictable, repeated travel passing through the weighing position with approximately constant velocity. For example, an oscillation at 0.2 Hz with 2 mm amplitude would

reach a peak velocity of  $2.5 \text{ mm s}^{-1}$ , with little down-time between repeat measurements.

## 6. CONCLUSIONS

We have shown that a syringe pump may be used as an automated volume regulator to controllably adjust the height of the piston in a pressure balance. This method can also be used to assist in maintaining a stable piston, and therefore coil, position in both the weighing and calibration modes of the MSL Kibble balance. We demonstrated constant velocity travel of the piston at  $1.7 \text{ mm s}^{-1}$  using two controlled start techniques to minimise unwanted oscillations. An oscillatory motion, working with the resonant behaviour of the pressure balance, also shows promise for the MSL Kibble balance calibration mode.

## ACKNOWLEDGEMENT

The authors wish to acknowledge useful discussions with and technical assistance from Joseph Borbely, Yin Hsien Fung, and Peter McDowall. The authors thank the reviewers for their insightful comments and suggestions for achieving constant velocity travel. This work was funded by the New Zealand Government.

## REFERENCES

- [1] I. A. Robinson, S. Schlamminger, The watt or Kibble balance: A technique for implementing the new SI definition of the unit of mass, *Metrologia*. 53 (2016) A46–A74. DOI: [10.1088/0026-1394/53/5/A46](https://doi.org/10.1088/0026-1394/53/5/A46)
- [2] C. M. Sutton, M. T. Clarkson, Y. H. Fung, The MSL Kibble Balance Weighing Mode, in: CPEM 2018 - Conference on Precision Electromagnetic Measurements, Institute of Electrical and Electronics Engineers Inc., 2018. DOI: [10.1109/CPEM.2018.8500889](https://doi.org/10.1109/CPEM.2018.8500889)
- [3] C. M. Sutton, The accurate generation of small gauge pressures using twin pressure balances, *Metrologia*. 23 (1987) 187–195. DOI: [10.1088/0026-1394/23/4/003](https://doi.org/10.1088/0026-1394/23/4/003)
- [4] C. M. Sutton, M.P. Fitzgerald, K. Carnegie, Improving the performance of the force comparator in a watt balance based on pressure balances, in: 2012 Conf. Precis. Electromagn. Meas., IEEE, 2012; pp. 468–469. DOI: [10.1109/CPEM.2012.6251006](https://doi.org/10.1109/CPEM.2012.6251006)
- [5] C. M. Sutton, M. T. Clarkson, A magnet system for the MSL watt balance, *Metrologia*. 51 (2014) S101–S106. DOI: [10.1088/0026-1394/51/2/S101](https://doi.org/10.1088/0026-1394/51/2/S101)
- [6] C. M. Sutton, An oscillatory dynamic mode for a watt balance, *Metrologia*. 46 (2009) 467–472. DOI: [10.1088/0026-1394/46/5/010](https://doi.org/10.1088/0026-1394/46/5/010)
- [7] C. M. Sutton, An improved mechanism for spinning the floating element of a pressure balance, *J. Phys. E*. 13 (1980) 825. DOI: [10.1088/0022-3735/13/8/007](https://doi.org/10.1088/0022-3735/13/8/007)
- [8] C. M. Sutton, M. P. Fitzgerald, D. G. Jack, An initial investigation of the damped resonant behaviour of gas-operated pressure balances, *Measurement*. 45 (2012) 2476–2478. DOI: [10.1016/j.measurement.2011.10.045](https://doi.org/10.1016/j.measurement.2011.10.045)
- [9] O. L. De Lange, J. Pierrus, Amplitude-Dependent Oscillations in Gases, *J. Nonlinear Math. Phys.* 8 (2001) 79–81. DOI: [10.2991/JNMP.2001.8.s.14](https://doi.org/10.2991/JNMP.2001.8.s.14)
- [10] S. Schlamminger, L. Chao, V. Lee, D. B. Newell, C. C. Speake, The crane operator's trick and other shenanigans with a pendulum, *Am. J. Phys.* 90 (2022) 169–176. DOI: [10.1119/10.0006965](https://doi.org/10.1119/10.0006965)
- [11] H. Ahmedov, N. B. Aşkin, B. Korutlu, R. Orhan, Preliminary Planck constant measurements via UME oscillating magnet Kibble balance, *Metrologia*. 55 (2018) 326–333. DOI: [10.1088/1681-7575/aab23d](https://doi.org/10.1088/1681-7575/aab23d)
- [12] C. Rothleitner, N. Rogge, S. Lin, S. Vasilyan, D. Knopf, F. Härtig, T. Fröhlich, Planck-Balance 1 (PB1) – a table-top Kibble balance for masses from 1 mg to 1 kg – current status, *ACTA IMEKO* 9 (2020) 5, pp. 47–52. DOI: [10.21014/acta\\_imeko.v9i5.937](https://doi.org/10.21014/acta_imeko.v9i5.937)
- [13] S. Vasilyan, N. Rogge, C. Rothleitner, S. Lin, I. Poroskun, D. Knopf, F. Härtig, T. Fröhlich, The progress in development of the Planck-Balance 2 (PB2): A tabletop Kibble balance for the mass calibration of E2 class weights, *Technisches Messen*. 88 (2021) 731–756. DOI: [10.1515/teme-2021-0101](https://doi.org/10.1515/teme-2021-0101)
- [14] R. R. A. Samodro, I. M. Choi, S. Y. Woo, S. J. Lee, A study on the pressure gradient effect due to a leak in a pressure calibration system, *Metrologia*. 49 (2012) 315–320. DOI: [10.1088/0026-1394/49/3/315](https://doi.org/10.1088/0026-1394/49/3/315)